

Probing in situ the formation mechanism of semi-conducting nanoplatelets by time resolved SAXS/WAXS (SC3629) : experimental report

Benjamin Abécassis

Experiment date and duration : April 5th to April 8th 2013. 8 shifts.

People present during the experiment : From LPS, Orsay : Benjamin Abécassis, Doru Constantin, Patrick Davidson. From LPEM, ESPCI, Paris : Sandrine Ithurria and Nicolas Lequeux.

Local contact : Diego Pontoni.

1 Goal of the experiment

This beamtime was allowed as a continuation of the SC3356 experiment in order to complete this experiment by supplementary data-sets. The goal was to confirm and deepen our previous findings and to run a certain number of tests and reference samples which relevance appeared during the previous experiment. Hence, the experimental set-up was the same as the one described in the SC3356 experiments and minimal change was brought to this aspect.

2 Overall assessment of the experiment

During the 3 days, all the experimental aspects relevant to the ID2 beamline and to the synchrotron in general worked smoothly. The beam has been stable for the whole course of the experiment and all the end-station elements operated correctly during the run. Hence, we used all the beamtime to acquire data without being troubled by side issues.

3 Experimental set-up

We used the same set-up as the one used in previous experiment SC3356 and a description of this system can be found in the relevant report. Briefly, we used a linkam hot-stage to heat a capillary containing the precursors at the right temperature.

A typical experiment happens as follow. First, the precursor solutions are mixed together and inserted in the glass capillary which is afterwards filled with dry argon

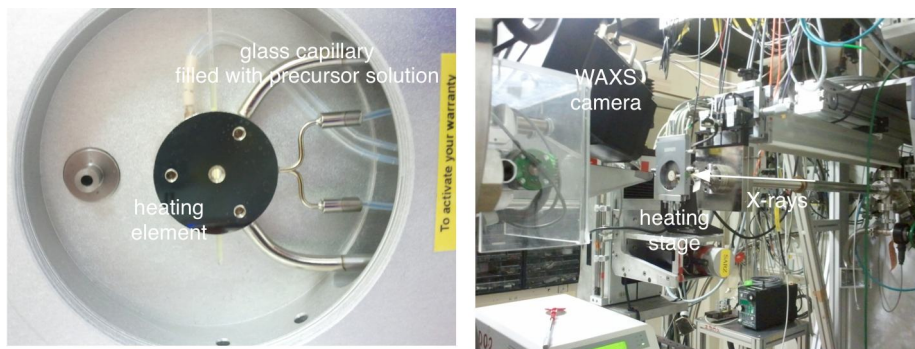


Figure 1: Left : Linkam hostage with a capillary filled with a precursor solution. The metal round part can be heated at the desired temperature and the X-rays go through the capillary through the hole at the center of the heated piece. Right : the hot stage set-up

and sealed with rubber. The capillary is then inserted in the hot-stage. Starting from ambient temperature, the capillary is then heated at the maximum heating rate while acquisition of SAXS patterns is triggered. Hence, we acquire SAXS patterns during the heating up of the solution and when the temperature reaches its maximum value. Typically, 500 SAXS/WAXS patterns are acquired during one experiment for a reaction time of 30 minutes.

4 Results

4.1 Reference samples

One of the goals of this experiment was to run reference samples such as solvent of the reaction (octadecene) at various temperatures and nanoparticle precursors to help the data treatment of SC3356. This task was perfectly achieved as described below.

4.1.1 Octadecene

The SAXS and WAXS profiles for pure octadecene before capillary background subtraction are presented in 2 for various temperatures ranging from 35 °C to 315 °C.

In the SAXS regime, we note that the intensity is increasing when the temperature is increasing. Theoretically, the intensity scattered when $q \rightarrow 0$ reads :

$$I = \rho^2 b^2 k T \chi_T \quad (1)$$

where ρ is the density, b is the scattering length density, k the boltzmann constant, T the temperature and χ_T the isothermal compressibility. On figure 3, we plot the octadecene SAXS profile after subtraction of the glass capillary background. The average value for different q -intervals and two different capillaries is also shown on the right panel

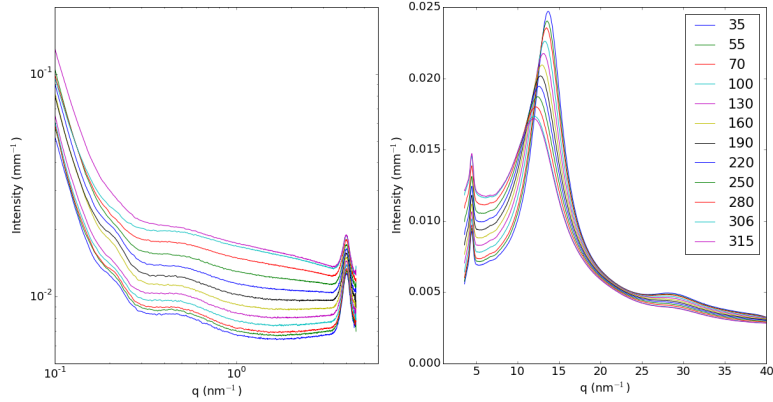


Figure 2: Scattering of pure octadecene at different temperatures for the SAXS (left) and WAXS (right) q -range before background subtraction. The small peak visible both in the SAXS and WAXS profiles at $q \simeq 4 \text{ nm}^{-1}$ is a background peak generated by the kapton LINKHAM stage windows.

of figure 3. It is clear that the intensity is not directly proportionnal to the temperature. Hence, the isothermal compressibility and/or the density of octadecene is changing with temperature in a non-linear fashion.

In the WAXS q -range (figure 1, right panel) we observe the broad and intense structure factor peak of the octadecene solvent. As temperature increases the peak broadens, decrease in intensity and the maximum shifts towards smaller q -values. On figure 3, we report the position of the peak as a function of temperature. A linear fit to the data yields the following relation between the position of the WAXS peak of the solvent (q_{WAXS} in nm^{-1} and temperature :

$$T = -158.88 \times q_{max} + 2490.195 \quad (2)$$

This relation can be used as an internal thermometer for every experiment. During a given temperature sequence we can check that the temperature in the capillary is actually the one which is imposed by the heating stage. To do so, we determine the position of the WAXS peak of octadecene and retrieve the temperature using equation 2. For a heating sequence from 100 to 240 °C, 4 shows the temperature retrieved from the WAXS peak position and the temperature imposed by the heating stage. The good agreement between the two curves shows that the

4.1.2 Glass capillary

The glass capillary intensity increases like q^{-4} in the SAXS regime but is negligible in the WAXS region. This contribution varies from one capillary to another and depends on the precise where the X-ray beam hits the capillary. Since we could not measure the

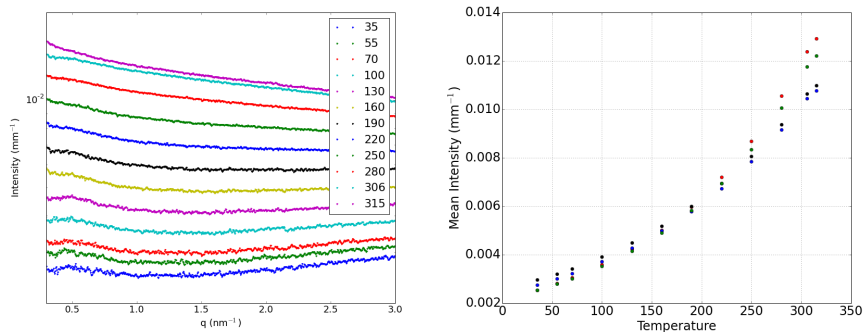


Figure 3: Left : $I(q)$ for pure octadecene at different temperatures subtracted of the background. Right : average value for different q ranges and for two different capillaries.

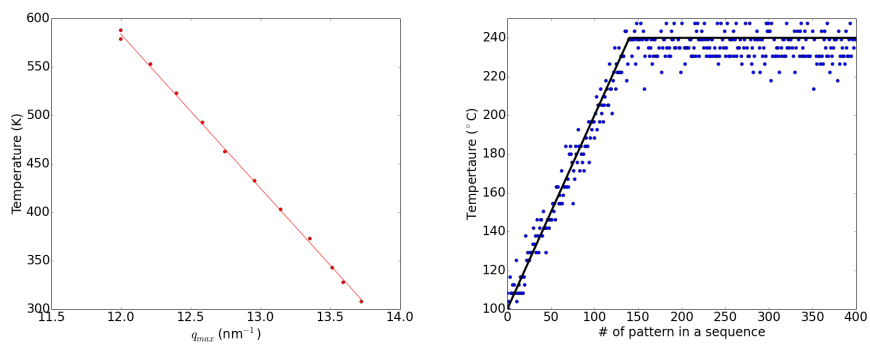


Figure 4: Left: position of the WAXS octadecene peak as a function of temperature. Right: User imposed temperature of the heating stage (black line) compared to the temperature retrieved from the position of the WAXS peak of the solvent.

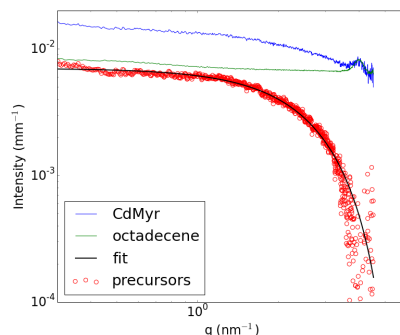


Figure 5: SAXS pattern of cadmium myristate: raw pattern and subtracted with octadecene. The fit corresponds to a monodisperse population of spheres with radius 0.67 nm.

signal independently, we used the first instants of the reaction to assess the contribution of the capillary.

4.1.3 Nanoparticle precursors

The nanoparticle precursors (cadmium myristate and selenium powder) can also have a scattering signal which we measured independently. We found that selenium powder dispersed in octadecene does not have a measurable contribution. This is due to the fact that selenium powder dispersed through low energy sonication in octadecene does not exhibit structuration at the scale probed by our SAXS experiment. On the contrary, it is likely that grains of size an order of magnitude larger than the maximum spatial dimension probed (roughly $\pi/q_{min} = 47$ nm) are present in solution and that they do not have a significant SAXS signal. Cadmium myristate, on the contrary, self-assembles in solution. Solutions of this compound in octadecene exhibit a significant scattering signal which depends on temperature (figure 5). For temperatures below 90°C , two peaks can be seen in the scattering patterns at wavevectors $q=0.084$ and 0.01366 nm^{-1} . These corresponds to the two orders of a lamellar structure with a 4 nm period. When temperature increases, the peaks disappear and the intensity scattered at low- q decreases to reach a value close to the one of octadecene. However, there is still a small scattering signal which comes out of the solvent even when the lamellar phase has melt. At 240°C , it can be fitted to a population of monodisperse spheres with a radius of $r_0 = 0.6790 \pm 0.0609$ nm. The fit is visible on 5.

This small signal is due to the X-ray scattering contrast between the head of the surfactant (cadmium atom bonded to a carboxylic acid group) which is rich in electron and the aliphatic tail which has a lower electron density.

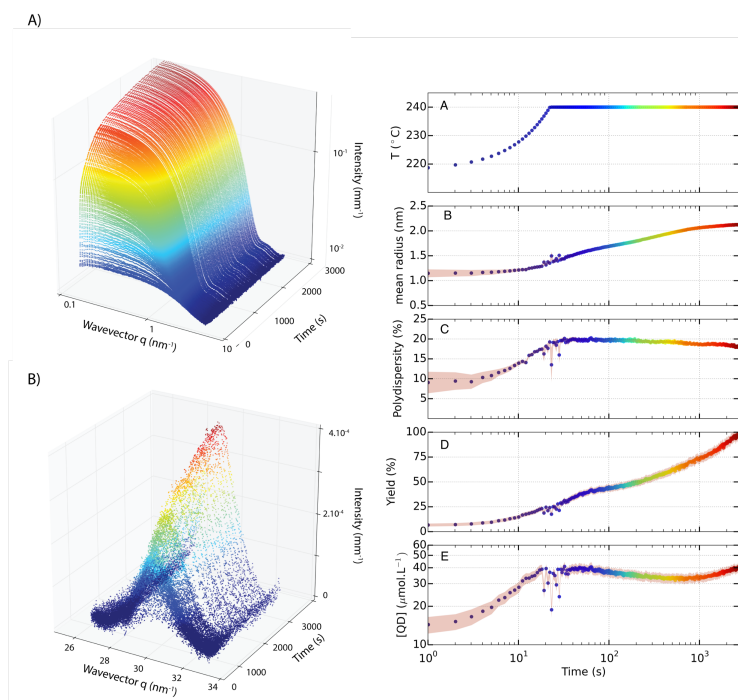


Figure 6: Results of time resolved in situ small angle X-ray scattering (SAXS) experiments for CdSe nanospheres (quantum dots). Left: SAXS and WAXS patterns as a function of time during the formation of the quantum dots. Right: Results of the Monte Carlo fits showing the evolution of radius and concentration in CdSe nanoparticles as a function of time. The colors of the points correspond to the color of the SAXS diagram on the left. The temperature increases with time at 1°C per second reaching 240°C at 140 s.

4.2 Quantum Dots

Significant results had been obtained during the previous experiment on the nucleation and growth of quantum dots in solution. The present experiment helped us to vary the experimental conditions and to reproduce previous funding. The results of these experiments and the subsequent data treatment has recently been published in Nano Letters.

Briefly, we fitted the data using a Monte Carlo technique and measured the concentration in nanoparticles, the mean radius and the polydispersity during the formation of the growth (figure 6). We redirect the interested reader the to original publication and to the supplementary materials where all the data treatment and interpretations are detailed.¹

¹<http://pubs.acs.org/doi/abs/10.1021/acs.nanolett.5b00199>

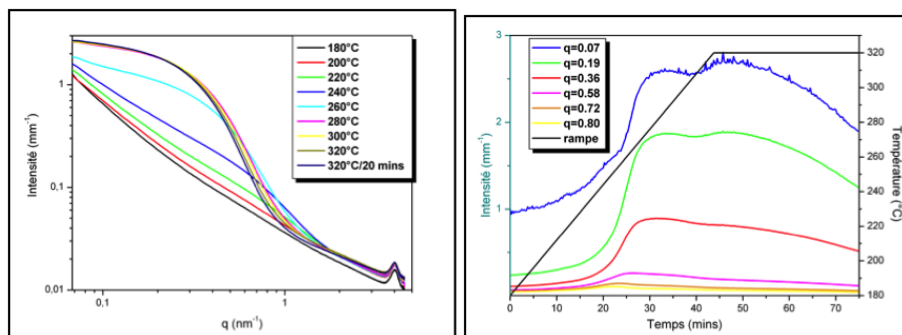


Figure 7: Evolution of SAXS pattern during the formation of Fe_2O_3 nanoparticle.

4.3 Iron oxide nanoparticles

In the framework of Cyril Garnero's internship, we also investigated the formation mechanism of iron oxide nanoparticles synthesized through the thermolysis of iron oleate at high temperature (318°C). Typical SAXS pattern evolution are shown on figure 7 and show a significant evolution of the scattered intensity as the nanoparticle appear. However, the iron precursor has a significant contribution and certainly self-assembles into polymeric species which hampers the elucidation of the first stages of the reaction. Considering this and also the fact that important results have been obtained on the quantum wells (see next section), we placed a lower priority in the advanced data treatment of this part of the experiment.

4.4 Quantum wells

We have studied the formation mechanism of colloidal quantum wells. We ran 15 kinetic sequences with varying the precursors concentration, temperature variations and q-range. We are currently treating these data along with those acquired during SC3356. In the SAXS part we see very important variations of the scattered intensity with some parts of the spectra exhibiting q^{-2} behavior indicating flat objects (figure 8). Complementary TEM experiments have shown that under these experimental conditions, the platelets roll under the constraints of the ligand. This is visible in the SAXS pattern as oscillations at small wave vectors corresponding to the radius of curvature. To deal with this, we are currently calculating theoretically the form factors corresponding to these shapes. In the WAXS diagram, we see large evolution of the diffraction peaks which we will quantify in order to obtain the size of the crystallographic domains in the different directions.

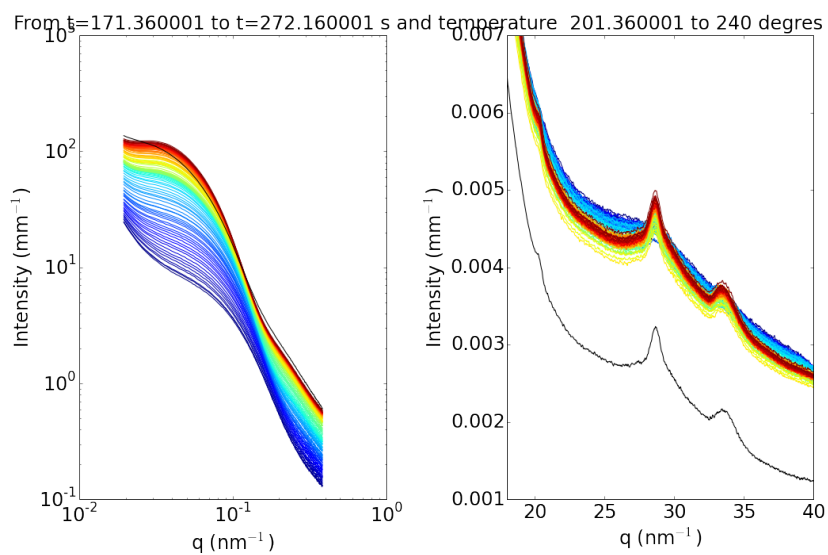


Figure 8: Evolution of the SAXS and WAXS intensity during the formation of colloidal quantum wells Left: SAXS patterns. Notice the q^{-2} slope which extends towards smaller q as the reaction goes on. Right: WAXS patterns showing the crystalline nature of the nano platelets. In both case, the curve in black is the final state of the sequence.

5 Conclusion and perspectives

In conclusion, we have obtained during these two runs on ID2 (SC3356 and SC3629) significant results on the formation mechanism of quantum dots and wells. We have demonstrated the feasibility of these high temperature experiments. On the quantum dot part, we published a paper in a high impact journal. Subsequent work will deal with combined UV-VIS/SAXS measurements and will be the subject of forthcoming proposals. Concerning the quantum wells, a lot of interesting data have been acquired and preliminary data treatment show that important results will be obtained in the coming months.